European Radiology (2019) 29:401–410
https://doi.org/10.1007/s00330-018-5559-z

GASTROINTESTINAL

LI-RADS v2014 categorization of hepatocellular carcinoma: Intraindividual comparison between gadopentetate dimeglumine-enhanced MRI and gadoxetic acid-enhanced MRI

Ji Soo Song[1,2,3] · Eun Jung Choi[1,2,3] · Seung Bae Hwang[1,2,3] · Hong Pil Hwang[4] · HyeMi Choi[5]

Received: 17 March 2018 / Revised: 12 May 2018 / Accepted: 23 May 2018 / Published online: 19 June 2018

Abstract

Objectives To use Liver Imaging Reporting and Data System (LI-RADS) categorization and features of hepatocellular carcinomas (HCCs) to intraindividually compare gadopentetate dimeglumine-enhanced magnetic resonance imaging (Gd-DTPA-MRI) and gadoxetic acid-enhanced MRI (Gd-EOB-MRI), before and after applying modified major features.

Methods Of 77 HCCs in 64 patients analysed, 17 HCCs were confirmed histopathologically and 46 patients had cirrhosis. Gd-EOB-MRI and Gd-DTPA-MRI were evaluated for the presence of major and ancillary features by two radiologists. LI-RADS categorization was done for Gd-DTPA-MRI (LI-RADS-DTPA) and for Gd-EOB-MRI before and after applying modified major features (hepatobiliary phase [HBP] hypointensity as an additional major feature, LI-RADS-EOBm1; HBP hypointense rim as capsule appearance, LI-RADS-EOBm2; and transitional phase [TP] hypointensity as washout appearance, LI-RADS-EOBm3). Sensitivities of LR-5 categorization for the diagnosis of HCC were compared.

Results Washout (p=0.012) and capsule appearance (p<0.001) were less frequently observed on Gd-EOB-MRI. Sensitivity for LR-5 categorization was significantly higher with LI-RADS-DTPA compared with LI-RADS-EOB (p=0.001) and LI-RADS-EOBm2 (p=0.004), while sensitivity for LR-5 categorization with LI-RADS-EOBm1 (p=0.210) and LI-RADS-EOBm3 (p=0.727) was comparable.

Conclusion Modifying LI-RADS for use with Gd-EOB-MRI, such as applying HBP hypointensity as an additional major feature or using TP hypointensity as washout appearance, can improve the sensitivity for the detection of HCC.

Key Points

- *Adding HBP hypointensity as additional major feature improved sensitivity of LR-5 categorization.*
- *Adding TP hypointensity as modified washout appearance improved sensitivity of LR-5 categorization.*
- *Sensitivities for LR-5 classification were comparable between LI-RADS-DTPA, LI-RADS-EOBm1, and LI-RADS-EOBm3.*

Keywords Hepatocellular carcinoma · Liver · Magnetic resonance imaging · Diagnosis · Gadopentetate dimeglumine

Abbreviations

Gd-DTPA-MRI	Gadopentetate dimeglumine-enhanced MRI
Gd-EOB-MRI	Gadoxetic acid-enhanced MRI
HBP	Hepatobiliary phase
LI-RADS	Liver Imaging Reporting and Data System

✉ Ji Soo Song
pichgo@gmail.com

[1] Department of Radiology, Chonbuk National University Medical School and Hospital, 20 Geonji-ro, Deokjin-gu, Jeonju, Chonbuk 54907, South Korea

[2] Research Institute of Clinical Medicine of Chonbuk National University, Jeonju, South Korea

[3] Biomedical Research Institute of Chonbuk National University Hospital, Jeonju, South Korea

[4] Department of Surgery, Chonbuk National University Medical School, Jeonju, South Korea

[5] Department of Statistics, Research Institute of Applied Statistics, Chonbuk National University, Jeonju, South Korea

Introduction

According to the guidelines of the American Association for the Study of Liver Diseases (AASLD) and the European Association for the Study of the Liver (EASL), hepatocellular carcinoma (HCC) can be diagnosed based solely on imaging in high risk patients (e.g., cirrhosis, chronic hepatitis) when hepatic nodules larger than 1 centimetre (cm) show arterial phase hyper-enhancement followed by washout on the portal venous phase (PVP) and/or the delayed phase (DP) on dynamic computed tomography (CT) or magnetic resonance imaging (MRI) using extracellular contrast media (ECCM) [1, 2]. However, these guidelines are not sufficiently detailed to achieve uniform adherence by different radiologists, which may lead to confusion and inconsistency in clinical practice [3]. To address this issue, the Liver Imaging Reporting and Data System (LI-RADS) was developed by the American College of Radiology [3, 4].

LI-RADS assigns a categorization to a lesion according to its probability of HCC, ranging from LR-1 (definitely benign) to LR-5 (definitely HCC). This categorization incorporates both major and ancillary features. Major features include arterial hyper-enhancement, washout appearance, and capsule appearance, and are used primarily to categorize hepatic lesions. Ancillary features are used to upgrade a lesion's categorization (but not beyond LR-4) or downgrade a lesion's categorization. LI-RADS v2014 incorporated the use of hepatobiliary contrast agents, such as gadoxetic acid, as a means of detecting ancillary features. It is well known that hepatobiliary phase (HBP) imaging on gadoxetic acid-enhanced MRI (Gd-EOB-MRI) provides increased lesion-to-liver contrast, enabling early detection of small HCCs and increasing the diagnostic sensitivity of MRI as compared to ECCM-enhanced MRI (ECCM-MRI) [5–7]. Choi et al showed that the detection of arterial phase hyper-enhancement and HBP hypointensity significantly increased the sensitivity (without altering the specificity) of diagnosis of small HCCs (≤ 2 cm) compared with EASL criteria [8]. An et al suggested that considering the detection of a smooth hypointense rim surrounding the lesion in HBP imaging as a capsule appearance improved the ability to diagnose HCC [9]. However, HBP hypointensity and the appearance of a HBP hypointense rim are only regarded as ancillary features that may favour the diagnosis of HCC in LI-RADS. Several Asian guidelines allow use of both PVP and transitional phase (TP) of Gd-EOB-MRI for determination of the washout appearance, while most of the major international guidelines only allow use of PVP of Gd-EOB-MRI for this purpose [10, 11].

A number of studies have validated LI-RADS using images from ECCM-enhanced CT and/or MRI, but only a few studies used Gd-EOB-MRI to validate LI-RADS or compared this modality to ECCM-enhanced CT [4, 12–15]. We hypothesized that to optimize the use of LI-RADS with Gd-EOB-MRI, additional major features of HCC should be considered, specifically HBP hypointensity, HBP hypointense rim, or TP hypointensity. LI-RADS categorization cannot be upgraded from LR-4 to LR-5 with ancillary features, while the presence of two or more major features can upgrade a case to LR-5. To the best of our knowledge, there are no data comparing LI-RADS using ECCM- and Gd-EOB-MRI images. The purpose of this study was to compare the frequency of major imaging features of LI-RADS and LI-RADS categorization on images obtained using both ECCM- and Gd-EOB-MRI, and to investigate the possibility that ancillary features of Gd-EOB-MRI images can be used to upgrade LI-RADS categorization of a lesion to LR-5.

Materials and methods

The Institutional Review Board of our hospital approved this study and waived the requirement for informed consent. This was a retrospective study using previously published data [16]. From January 2009 to November 2009, 80 patients suspected of having HCCs or liver metastases based on prior CT or sonography were prospectively enrolled at our hospital to compare the diagnostic accuracy and sensitivity of Gd-EOB-MRI with double-contrast MRI, which combines gadopentetate dimeglumine-enhanced MRI (Gd-DTPA-MRI) and superparamagnetic iron-oxide-enhanced MRI for lesion detection. The prior study included 49 patients with 56 HCCs and compared the typical vascular enhancement patterns and capsule appearance of HCCs using three consecutive imaging studies: dynamic CT, Gd-DTPA-MRI, and Gd-EOB-MRI. This current study used this same sample; however, we did not exclude patients without a dynamic CT, and we focused on comparing LI-RADS categorization using Gd-DTPA-MRI and Gd-EOB-MRI.

MR imaging techniques

All MR examinations were performed using a 1.5-Tesla (T) MR system (MAGNETOM Symphony; Siemens Healthineers) equipped with an 8-channel body phase-array coil. We obtained two-dimensional gradient-echo (GRE) T1-weighted images with dual-echo acquisition (repetition time/echo times [TR/TE], 180/2.4-5.2 milliseconds [ms]; flip angle, 70°; matrix, 384 × 225; Field of View (FOV), 350 × 320 millimetres [mm]; slice thickness, 6 mm), fat-suppressed fast spin-echo (FSE) T2-weighted images (TR/TE, 3378-4800/68-76 ms; flip angle, 150°; matrix, 384 × 225; FOV, 350 × 320 mm; slice thickness, 6 mm). Three-dimensional dynamic fat-suppressed GRE T1-weighted images (TR/TE, 4.3/2.0 ms; flip angle, 12°; matrix, 256 × 133; FOV, 305 × 263 mm; slice thickness, 2.5-3.0 mm) were acquired using Gd-EOB-MRI (including dynamic phase and HBP) and Gd-DTPA-MRI (including just the dynamic phase). The delay after contrast material administration for arterial phase (AP) imaging was

determined using the MR fluoroscopic bolus detection technique (CARE Bolus; Siemens Healthineers). The mean delay times for the AP, PVP, and DP/TP were 20, 60, and 180 s, respectively. Using Gd-EOB-MRI, the HBP images were acquired at 10 and 20 min after the administration of contrast medium, and 20-min HBP images were used for image analysis. Each phase was acquired during the breath-hold period during end-expiration. Gadopentetate dimeglumine (Magnevist; Bayer Healthcare) and gadoxetic acid (Primovist, Eovist; Bayer Healthcare) were administered intravenously by using a standard weight-based dose of 0.1 millimole/kilogram ([mmol/kg] or 0.2 millilitres/kilogram [mL/kg]) and 0.025 mmol/kg (or 0.1 mL/kg) at a rate of 2 millilitres/second (mL/s) for the gadopentetate dimeglumine and 1 mL/s for the gadoxetic acid, both followed by a 20 mL saline flush.

Image analysis

Two abdominal radiologists (with 10 and 4 years of experience in abdominal imaging) who were aware of the study population and objectives independently analysed all of the MR images in two review sessions separated by 4 weeks. In the first session, Gd-DTPA-MRI images were evaluated by reviewer 1 and Gd-EOB-MRI images were evaluated by reviewer 2; this order was reversed in the second session. Reviewers were not blinded to the MR contrast agent used in the studies since they could detect the presence of HBP on Gd-EOB-MRI. The target nodules were marked by the study coordinator. Each lesion was evaluated for the presence or absence of major features (arterial phase hyper-enhancement, washout appearance, or capsule appearance) and ancillary features (hypointensity on the TP or HBP, mild–moderate T2 hyperintensity, restricted diffusion, distinctive rim, corona enhancement, HBP hypointense rim, mosaic architecture, nodule-in-nodule architecture, intralesional fat, lesional iron sparing, lesional fat sparing, and blood products) that may favour malignancy or benignity (homogeneous-marked T2 hyperintensity, homogeneous-marked T2 or T2* hypointensity, HBP isointensity, undistorted vessels, and parallel blood pool enhancement) during the first session. Nodule size was measured as the longest diameter on TP or HBP on Gd-EOB-MRI images. Since previous images were not provided in the analysis for comparison, threshold growth and visibility on ultrasound were not considered in LI-RADS categorization. After an initial independent review, any discordant imaging features between the two reviewers were resolved by consensus discussion during the second session.

For Gd-EOB-MRI, LI-RADS categorization was done four times. The first categorization was performed before applying the modified major features (LI-RADS-EOB) and the subsequent three categorizations were performed after applying the modified major features (LI-RADS-EOBm1, LI-RADS-EOBm2, and LI-RADS-EOBm3). The modified major features of LI-RADS-EOBm1 included arterial phase hyper-enhancement, washout appearance, capsule appearance, and HBP hypointensity. The modified major features of LI-RADS-EOBm2 included arterial phase hyper-enhancement, washout appearance, capsule appearance, and an HBP hypointense rim considered as modified capsule appearance. The modified major features of LI-RADS-EOBm3 included arterial phase hyper-enhancement, washout appearance, capsule appearance, and TP hypointensity as modified washout appearance. All definitions regarding the imaging features and principles behind the determination of LI-RADS categories were based on LI-RADS v2014 [3].

Statistical analysis

The frequencies of each major and modified major feature, except HBP hypointensity, were compared between Gd-DTPA-MRI and Gd-EOB-MRI using the McNemar test. Subgroup analysis was performed according to lesion size (<10 mm, 10–19 mm, ≥20 mm) determined by the mean value of the tumor diameter measurements of the two reviewers. Interobserver agreement was assessed using the kappa test. Agreement between Gd-DTPA-MRI and Gd-EOB-MRI for LI-RADS categorization was assessed using the kappa test. Kappa values were interpreted as follows: poor agreement, <0.20; fair, 0.20–0.39; moderate, 0.40–0.59; substantial, 0.60–0.79; and almost perfect, ≥ 0.80. Per-lesion sensitivities of LR-5 for the diagnosis of HCCs were compared between Gd-DTPA-MRI and Gd-EOB-MRI using the McNemar test.

All statistical analyses were performed using MedCalc version 13.0.0.0 (MedCalc Software) or SPSS version 22 (SPSS Inc.). A p value of < 0.05 was considered statistically significant.

Results

Patients

The current study included 77 HCCs (2.0 ± 1.2 cm; range, 0.8 – 9.9 cm) in 64 patients (53 males and 11 females; mean age, 57.6 years; range, 35 – 76 years) with chronic hepatitis or cirrhosis who underwent two MR examinations: Gd-EOB-MRI and sequentially acquired Gd-DTPA-MRI. The interval between the two MR examinations ranged from 1 to 18 days (mean interval, 5 days). The causes of chronic hepatitis or liver cirrhosis were as follows: hepatitis B (n = 35), hepatitis C (n = 7), alcohol abuse (n = 20), and cryptogenic (n = 2). Forty-six patients had liver cirrhosis (Child-Pugh class A/B = 41/5).

Lesion confirmation

Of the 77 nodules, 17 nodules were confirmed as HCC through histopathology by surgical resection, and 60 nodules

were diagnosed by the typical enhancement pattern of HCC according to the 2010 AASLD guidelines (arterial phase hyper-enhancement and PVP or DP washout on dynamic CT and/or Gd-DTPA-MRI) [2]. Of the 60 nodules, 47 were treated by transarterial chemoembolization; and characteristic angiographic findings as well as compact lipiodol uptake were confirmed on a follow-up CT. Of the remaining 13 nodules, which were all larger than 1 cm with a typical HCC enhancement pattern, eight nodules were treated by radiofrequency ablation, and five nodules had no follow-up data. Of 55 nodules treated either by transarterial chemoembolization or radiofrequency ablation, 26 nodules (47.3 %) showed local tumor progression on follow-up.

Comparison of the frequencies of major features and modified major features

Among the major features, the percentage of cases demonstrating arterial hyper-enhancement was not significantly different between Gd-DTPA-MRI and Gd-EOB-MRI (98.7% for both, respectively). Washout appearance (76.6% and 61.0% respectively, $p = 0.012$) and capsule appearance (75.3% and 50.7% respectively, $p < 0.001$) were less frequently demonstrated on Gd-EOB-MRI than on Gd-DTPA-MRI (Table 1). The number of HCC cases by tumor size were as follows: < 10 mm, $n = 3$; 10-19 mm, $n = 43$; ≥ 20 mm, $n = 31$. In the subgroup analysis, significant differences were present for washout appearance in the tumor size group of ≥ 20 mm ($p = 0.008$), and for capsule appearance in the tumor size groups of 10-19 mm ($p = 0.007$) and ≥ 20 mm ($p = 0.002$, see Table 1). Gd-EOB-MRI was superior to Gd-DTPA-MRI in detecting washout appearance when considering TP hypointensity as modified washout appearance for all tumor sizes (76.6 % vs 89.6 %, $p = 0.002$), as well as in the 10-19 mm size group (65.1% vs 83.7%, $p = 0.005$; Fig. 1). When applying HBP hypointense rim as a modified capsule appearance, Gd-DTPA-MRI demonstrated capsule appearance more frequently than Gd-EOB-MRI for all tumor sizes (75.3% vs. 54.6%, $p < 0.001$), as well as in the tumor size groups of 10-19 mm (70.0% vs. 48.8%, $p = 0.007$) and ≥ 20 mm (90.3% vs. 67.7%, $p = 0.020$). Only seven HCCs showed an HBP hypointense rim (Table 1, Fig, 2). The kappa values between the two radiologists yielded fair to almost perfect agreement (Table 2).

Table 1 Frequencies of major imaging features and modified major features

Major features	Gd-DTPA-MRI	Gd-EOB-MRI	*p* value
Arterial hyper-enhancement			
All tumor sizes	98.7 (76/77)	98.7 (76/77)	N/A[1]
< 10 mm	100.0 (3/3)	100.0 (3/3)	N/A[1]
10-19 mm	100.0 (43/43)	100.0 (43/43)	N/A[1]
≥ 20 mm	96.8 (30/31)	96.8 (30/31)	N/A[1]
Washout appearance			
All tumor sizes	76.6 (59/77)	61.0 (47/77)	0.012
< 10 mm	33.3 (1/3)	100.0 (3/3)	N/A[2]
10-19 mm	65.1 (28/43)	51.2 (22/43)	0.109
≥ 20 mm	96.8 (30/31)	71.0 (22/31)	0.008
Capsule appearance			
All tumor sizes	75.3 (58/77)	50.7 (39/77)	< 0.001
< 10 mm	0 (0/3)	0 (0/3)	N/A[1]
10-19 mm	70.0 (30/43)	48.8 (21/43)	0.007
≥ 20 mm	90.3 (28/31)	58.1 (18/31)	0.002
Modified washout appearance*			
All tumor sizes	76.6 (59/77)	89.6 (69/77)	0.002
< 10 mm	33.3 (1/3)	100.0 (3/3)	N/A[2]
10-19 mm	65.1 (28/43)	83.7 (36/43)	0.005
≥ 20 mm	96.8 (30/31)	96.8 (30/31)	N/A[1]
Modified capsule appearance**			
All tumor sizes	75.3 (58/77)	54.6 (42/77)	< 0.001
< 10 mm	0 (0/3)	0 (0/3)	N/A[1]
10-19 mm	70.0 (30/43)	48.8 (21/43)	0.007
≥ 20 mm	90.3 (28/31)	67.7 (21/31)	0.020

Note.–Data are percentages, and raw data are in parentheses. *P* values were determined with McNemar test. PVP=portal venous phase, DP=delayed phase, TP=transitional phase

N/A[1] McNemar test was not conducted because there were no discordant pairs

N/A[2] McNemar test was not conducted because there were zero negative observations in Gd-EOB-MRI

* TP hypointensity also considered as a washout appearance on Gd-EOB-MRI

** HBP hypointense rim also considered as a capsule appearance on Gd-EOB-MRI

LI-RADS categorization and sensitivities of LR-5 using Gd-DTPA-MRI and Gd-EOB-MRI

None of the observations were categorized as LR-1 or LR-2. The agreement of LI-RADS categorization between Gd-DTPA-MRI (LI-RADS-DTPA) and LI-RADS-EOB was moderate (k = 0.58). The agreement between LI-RADS-DTPA and LI-RADS-EOBm1 (k = 0.52) and between LI-RADS-DTPA and LI-RADS-EOBm2 (k = 0.58) was also moderate. There was substantial agreement between LI-RADS-DTPA and LI-RADS-EOBm3 ([k = 0.75], Table 3).

The sensitivities of an assignment of LR-5 for the diagnosis of HCC were significantly higher on LI-RADS-DTPA compared with both LI-RADS-EOB (66.2% vs 48.1%, $p = 0.001$) and LI-RADS-EOBm2 (66.2% vs 50.6%, $p = 0.004$). The sensitivities of an assignment of LR-5 for the diagnosis of HCC did not differ significantly using LI-RADS-EOBm1 (74.0%, $p = 0.210$) or LI-RADS-EOBm3 (63.6%, $p = 0.727$) compared with LI-RADS-DTPA (66.2%; See Table 3 and Fig. 3).

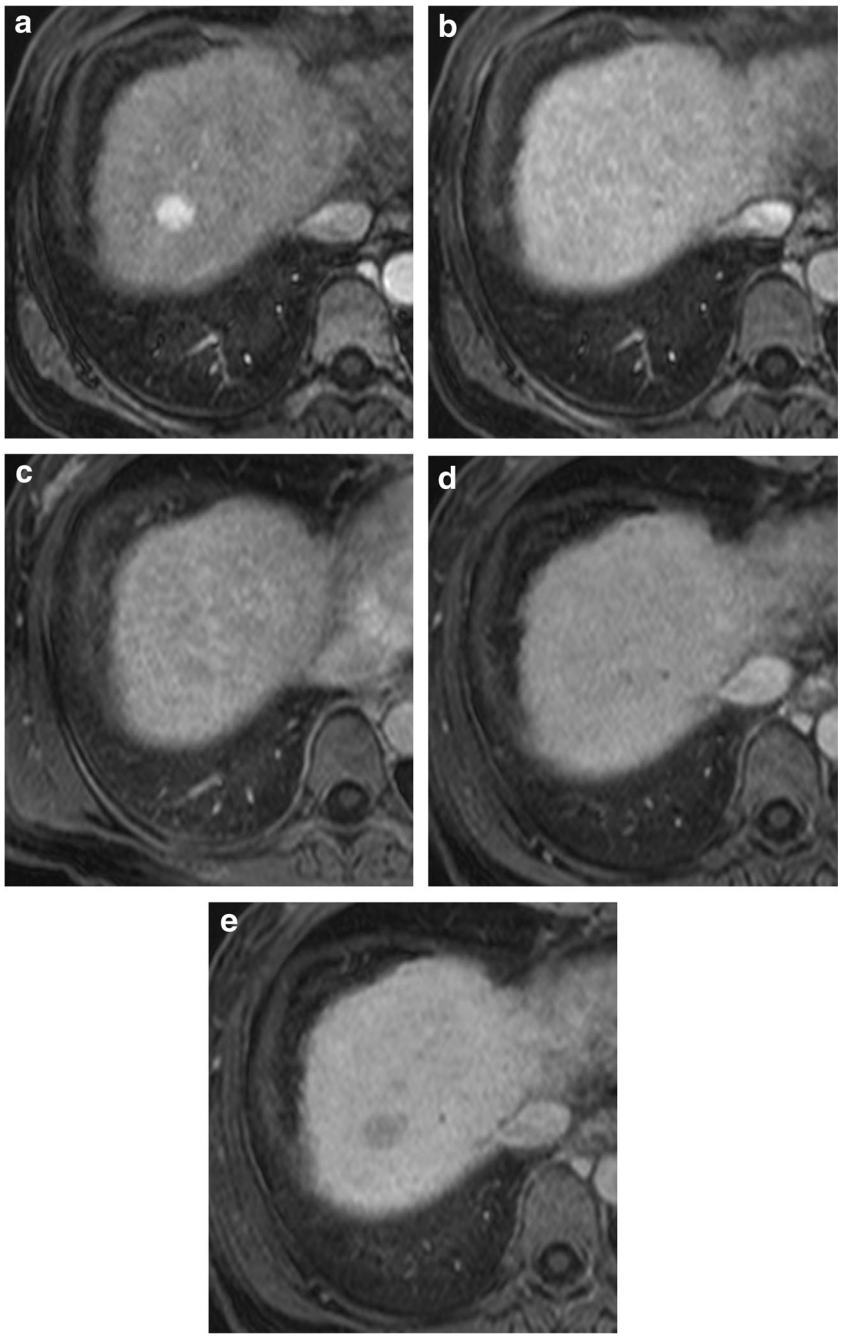

Fig. 1 1.5 cm sized hepatocellular carcinoma in segment VIII in a 53-year-old female with cirrhosis. Gadopentetate dimeglumine-enhanced MRI shows arterial phase hyper-enhancement (**a**) followed by isointensity in the portal venous phase (**b**) and subtle hypointensity in the delayed phase (**c**, washout appearance). Gadoxetic acid-enhanced MRI shows isointensity in the portal venous phase (**d**) and hypointensity in the transitional phase (**e**, modified washout appearance)

Discussion

Our study demonstrated that washout appearance and capsule appearance were less frequently observed on images obtained from Gd-EOB-MRI than from Gd-DTPA-MRI. After applying the modified washout appearance, which considered TP hypointensity as washout appearance, Gd-EOB-MRI demonstrated washout appearance significantly better than Gd-DTPA-MRI. The addition of the modified capsule appearance (HBP hypointense rim considered as capsule appearance) did not affect the frequency of the capsule appearance on Gd-DTPA-MRI images. The sensitivity of LR-5 category designation for the diagnosis of HCC was significantly lower when assigned using LI-RADS-EOB and LI-RADS-EOBm2 than when assigned using LI-RADS-DTPA. However, the sensitivity of LR-5 category designation was comparable or even better when assigned using LI-RADS-EOBm1 (hypointensity at HBP as additional major feature) and LI-RADS-EOBm3 (considering TP hypointensity as washout appearance) than when assigned using LI-RADS-DTPA.

There were 23 HCCs that did not show washout appearance on PVP but that did demonstrate HBP hypointensity. Of

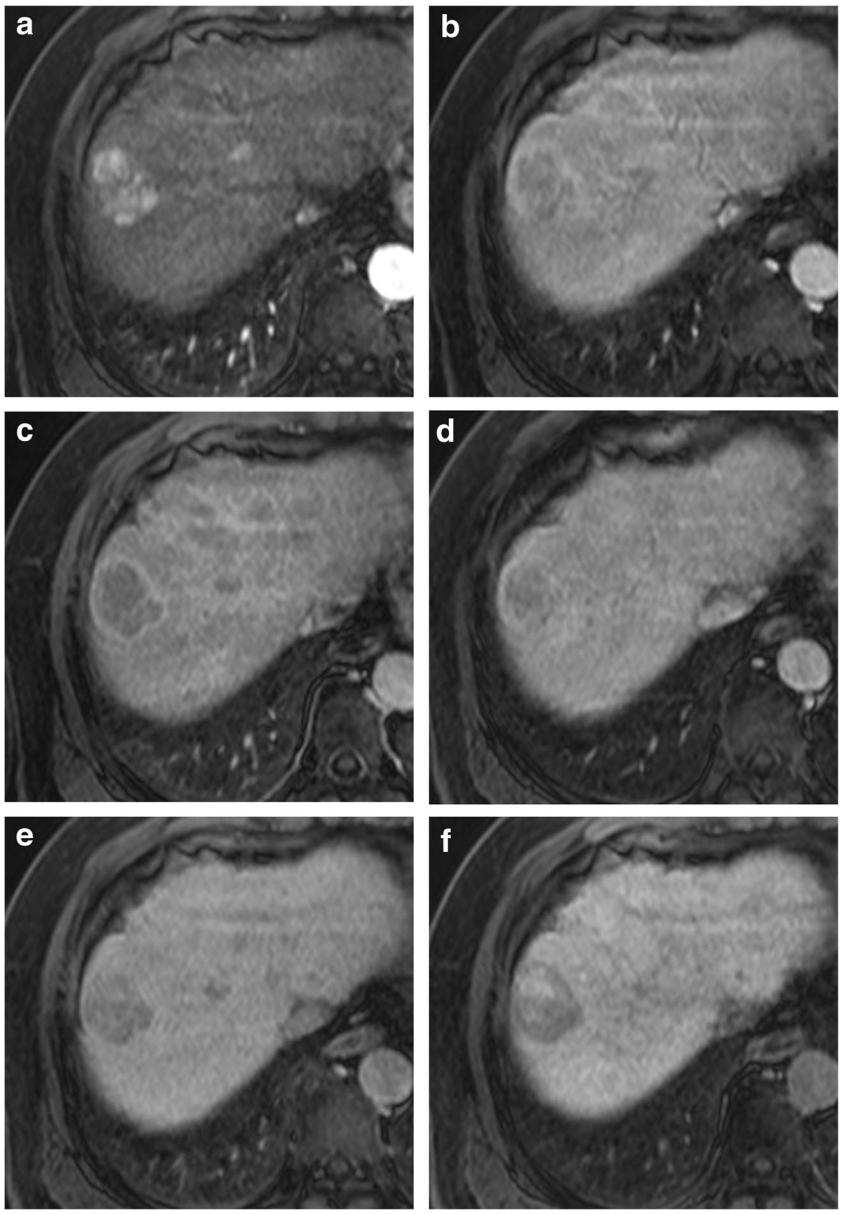

Fig. 2 3.5 cm sized hepatocellular carcinoma in segment VIII in a 64-year-old male with cirrhosis. Gadopentetate dimeglumine-enhanced MRI shows arterial phase hyper-enhancement (**a**) followed by washout appearance in the portal venous phase (**b**) and delayed phase (**c**). Capsule appearance is present in the delayed phase. Gadoxetic acid-enhanced MRI shows washout appearance in the portal venous phase (**d**) and hypointensity in the transitional phase (**e**, modified washout appearance). In the hepatobiliary phase (**f**), the lesion shows heterogeneous hyperintensity with hypointense rim (modified capsule appearance)

these, 11 HCCs could be upgraded to LR-5 from LR-4 when using LI-RADS-EOBm1. HBP hypointensity is one of the well-known features of HCC lesions, and its presence increases the sensitivity for the diagnosis of HCC [17]. However, the specificities of HBP hypointensity varies widely among many studies, ranging from 33% to 96.7% [7, 18, 19]. One study demonstrated that the presence of arterial hyper-enhancement and HBP hypointensity may increase the diagnostic sensitivity for detecting small HCCs (≤ 2 cm), as compared to the EASL criteria [8]. When combined with major and ancillary features of LI-RADS, HBP hypointensity can improve the sensitivity for diagnosing HCC without altering the specificity.

A prior study also demonstrated that adding HBP hypointense rim as capsule appearance as a feature of LI-RADS could increase the sensitivity (83% vs 72.7%, $p < 0.001$) and accuracy (84.1% vs 75.1%, $p < 0.001$) while retaining a specificity of 91.5%. Overall, the prevalence of the conventional capsule appearance and the HBP hypointense rim in this prior study was 52.4% and 71.5%, respectively [9]. In our study, although the prevalence of capsule appearance was in the range of other previous studies (24 – 57.8%), only seven HCCs showed a HBP hypointense rim. We assume that this may be due to our use of a different study design and inclusion criteria, a smaller sample size, and the use of a 1.5 T MR system, all of which may have led to a different threshold detection in this finding.

The frequency of the conventional washout appearance was significantly lower in Gd-EOB-MRI as compared to Gd-DTPA-MRI for all lesions, as well as in subgroups of

Table 2 Interobserver agreement of two radiologists for major and ancillary features

	Gd-DTPA-MRI	Gd-EOB-MRI
Major features		
Arterial hyper-enhancement	1	1
Washout appearance on PVP	0.73 (0.58, 0.89)	0.82 (0.68, 0.95)
Washout appearance on DP/TP	0.55 (0.34, 0.77)	0.54 (0.28, 0.80)
Capsule appearance	0.69 (0.51, 0.88)	0.71 (0.56, 0.87)
Ancillary features that favour malignancy		
HBP hypointensity	N/A	0.93 (0.81, 1.00)
HBP hypointense rim	N/A	0.78 (0.54, 1.00)
Mild to moderate T2 hyperintensity	0.58 (0.30, 0.86)	0.62 (0.35, 0.90)
Distinctive rim	0.51 (0.23, 0.79)	0.51 (0.23, 0.79)
Corona enhancement	0.36 (0.06, 0.66)	0.27 (0.00, 0.55)
Mosaic architecture	0.67 (0.49, 0.85)	0.66 (0.47, 0.84)
Nodule-in-nodule appearance	0.79 (0.40, 1.00)	0.47 (0.03, 0.91)
Intralesional fat	0.63 (0.34, 0.93)	0.63 (0.34, 0.93)
Lesional iron sparing	0.49 (-0.11, 1.00)	0.49 (-0.11, 1.00)
Lesional fat sparing	1	1
Blood products	0.65 (0.21, 1.00)	0.65 (0.21, 1.00)
Ancillary features that favour benignity*	1	1

Note.–Data are kappa values, and 95% confidence interval are in parentheses. PVP=portal venous phase, DP=delayed phase, TP=transitional phase, HBP=hepatobiliary phase

* All showed almost perfect agreement (kappa=1), except HBP isointensity (kappa=0.75 [0.48, 1.00]), respectively

lesions measuring 10-19 mm and ≥ 20 mm. However, the frequency of the modified washout appearance was significantly higher in images obtained from Gd-EOB-MRI for all tumor sizes, as well as in the 10-19 mm size group. Joo et al reported that using only PVP on Gd-EOB-MRI to assess HCC washout appearance was associated with a high specificity (97.9%) and a reasonable sensitivity (70.9%) [20]. In our study, when washout appearance was only assessed on PVP, the sensitivity was 48.1% (37/77). As compared to Joo's study, the mean size of HCCs in our study was smaller (mean, 2.0 cm vs 3.5 cm; range, 0.8-9.9 cm vs 1-21 cm), and we used LI-RADS as our diagnostic algorithm (whereas Joo used AASLD). Interestingly, in Joo's subgroup analysis of HCCs ≤ 2 cm, the sensitivity associated with using only PVP on Gd-EOB-MRI decreased to 55.7%, which is similar to ours. After applying the modified washout appearance, the sensitivity of LR-5 for diagnosing HCC increased to 63.6%, which was similar to that of LI-RADS-DTPA (66.2%).

Table 3 Comparison of overall LI-RADS categorization and sensitivities of LR-5

	DTPA	EOB	*p* value[1]	k[1]	EOBm1	*p* value[2]	k[2]	EOBm2	*p* value[3]	k[3]	EOBm3	*P* value[4]	k[4]
LR-5	66.2 (51/77)	48.1 (37/77)	0.001	0.58	74.0 (57/77)	0.210	0.52	50.6 (39/77)	0.004	0.58	63.6 (49/77)	0.727	0.75
LR-4	32.5 (25/77)	50.6 (39/77)			24.7 (19/77)			48.1 (37/77)			35.1 (27/77)		
LR-3	1.3 (1/77)	1.3 (1/77)			1.3 (1/77)			1.3 (1/77)			1.3 (1/77)		

Note.–Data are percentages, and raw data are in parentheses. *P* values were determined with McNemar test. DTPA=LI-RADS categorization with Gd-DTPA-MRI, EOB=LI-RADS categorization with Gd-EOB-MRI, EOBm1=modified LI-RADS categorization with Gd-EOB-MRI (HBP hypointensity as additional major feature), EOBm2=modified LI-RADS categorization with Gd-EOB-MRI (HBP hypointense rim as capsule appearance), EOBm3=modified LI-RADS categorization with Gd-EOB-MRI (TP hypointensity as washout appearance)

[1] DTPA vs EOB

[2] DTPA vs EOBm1

[3] DTPA vs EOBm2

[4] DTPA vs EOBm3

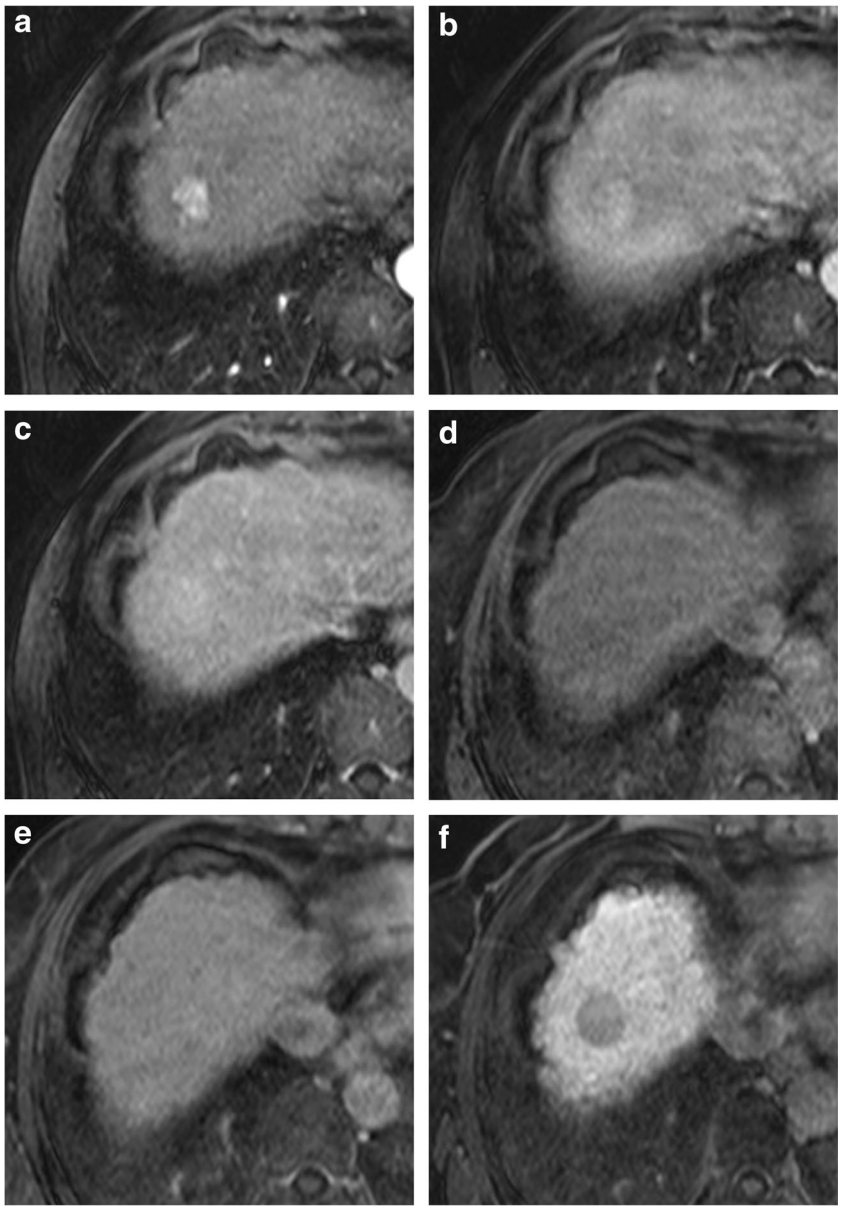

Fig. 3 Surgically confirmed 2.1 cm sized hepatocellular carcinoma in segment VIII in a 62-year-old female with cirrhosis. Gadopentetate dimeglumine-enhanced MRI shows arterial phase hyperintensity (**a**) followed by subtle hyperintensity in the portal venous phase (**b**) and isointensity in the delayed phase (**c**). The lesion was categorized as LR-4. Gadoxetic acid-enhanced MRI shows isointensity in the portal venous (**d**) and transitional phase (**e**). In the hepatobiliary phase (HBP), the lesion shows hypointensity (**f**). The lesion was categorized as LR-4. However, when considering HBP hypointensity as additional major feature (LI-RADS-EOBm1), the lesion was categorized as LR-5

Although we could not evaluate specificity in the current study, considering TP hypointensity as washout appearance increases the sensitivity to a level similar to that of the current LI-RADS with ECCM.

Many studies have demonstrated substantial discordance between the accuracy of LI-RADS using MRI and MDCT [21, 22]. Joo et al showed that LR-4 categorization occurred more frequently when using Gd-EOB-MRI than with MDCT, as ancillary features detected on Gd-EOB-MRI frequently yielded images that upgraded the categorization from LR-3 to LR-4 [12]. Since we compared both types of MRI using different contrast media, we found less discordance in categorization between the images. The lower sensitivity of LI-RADS-EOB in our study compared to that reported in Joo et al (63.4% vs 48.1%) may be attributed mainly to the smaller mean size of the HCC lesions in our study; 40% (31/77) of HCCs were ≥ 2 cm in our study as compared to 71% (154/216) in the previous study [12].

Another prior study demonstrated that the combination of Gd-EOB-MRI and diffusion-weighted imaging might improve the detection of major features of LI-RADS [13]. Cha et al compared the diagnostic performance of LI-RADS and a modified LI-RADS, which used features favouring HCC detected using HBP and restricted diffusion on diffusion-weighted imaging as a major feature, rather than threshold growth [13]. Although there was no significant difference in pairwise comparisons of receiver operating characteristic (ROC) curves, the sensitivity, specificity, and area under the ROC curve were higher with the modified LI-RADS. The authors concluded that the combination of imaging features

favouring HCC detected using HBP, and restricted diffusion might be able to act as a major feature regardless of the findings on previous imaging studies. In the current study, 15 HCCs had an LR-5 categorization using LI-RADS-DTPA but an LR-4 categorization using LI-RADS-EOB. Of these 15 HCCs, ten were 10-19 mm and most had either washout appearance or capsule appearance. The remaining five HCCs in this group were ≥ 20 mm and lacked both washout appearance and capsule appearance. However, all 15 HCCs had either TP hypointensity or HBP hypointensity, which resulted in an upgrade to a categorization of LR-5 on LI-RADS-EOBm1 and LI-RADS-EOBm3. Since only seven HCCs showed an HBP hypointense rim, and of this number, four HCCs also showed a conventional capsule appearance, there was only a minor change in LI-RADS-EOBm2 categorization. An advantage of our study is that it is the first evaluation comparing the use of LI-RADS using images obtained from ECCM-MRI and Gd-EOB-MRI. The results of our study, combined with prior research, suggest that there is a need for modification of LI-RADS when used with images obtained using Gd-EOB-MRI [12, 13].

Our study has several limitations that may impact generalizability. First, the biggest limitation of our study was that an analysis of specificity was not possible, since non-HCC lesions, such as benign nodules, borderline cirrhotic nodules, hypovascular HCCs, or cholangiocarcinomas, were not included. Instead, we only included HCCs in order to compare the sensitivities of LI-RADS on ECCM-MRI and Gd-EOB-MRI. Therefore, further studies are warranted to assess the specificity of LI-RADS on Gd-EOB-MRI with and without modification. Second, the use of a retrospective design may have introduced a selection bias. Since most of the lesions met the criteria for HCC based on 2010 AASLD guidelines, the results of our study may not be generalizable to a screening population to assess lesions that do not meet the 2010 AASLD guidelines for HCC. Third, most HCCs were not histologically confirmed; however, the majority of patients at high risk of HCC are managed based on imaging findings and rarely require biopsy for management [2]. Fourth, we used a 1.5-T MR without diffusion-weighted images, which may have made our results less comparable to data obtained from 3-T MR or with diffusion-weighted imaging. Finally, the study design may not have reflected actual clinical practice in which multiple imaging modalities are often used in combination to diagnose HCC.

In conclusion, our study found that modification of LI-RADS can improve the diagnostic sensitivity in detecting HCC using Gd-EOB-MRI, although further studies are necessary to investigate diagnostic specificity regarding any modification to LI-RADS. When applying HBP hypointensity as an additional major feature or modified washout appearance to LI-RADS, the sensitivities of LR-5 categorization can be improved to be comparable or better than in LI-RADS-DTPA. This suggests that modification of LI-RADS may help increase the accuracy in detecting HCC, although future prospective studies with a larger sample size that includes non-HCC lesions is warranted to validate our study results.

Acknowledgements The authors thank Wade Martin of Emareye Medical Editing Service for his assistance in editing the article.

Funding This research was supported by "Research Base Construction Fund Support Program" funded by Chonbuk National University in 2018.

Compliance with ethical standards

Guarantor The scientific guarantor of this publication is Ji Soo Song.

Conflict of interest The authors of this manuscript declare no relationships with any companies, whose products or services may be related to the subject matter of the article.

Statistics and biometry Statistical analysis was performed by Dr. HyeMi Choi, who is an expert in statistics.

Informed consent Written informed consent was waived by the Institutional Review Board.

Ethical approval Institutional Review Board approval was obtained.

Study subjects or cohorts overlap Data from the 49 patients were published previously (Kim et al Acta Radiol. https://doi.org/10.1177/0284185117728534). From January 2009 to November 2009, 80 patients were prospectively enrolled to compare the diagnostic accuracy and sensitivity of Gd-EOB-MRI with double-contrast MRI, which combined Gd-DTPA-MRI and superparamagnetic iron-oxide-enhanced MRI, for HCC detection. In this study, we did not exclude patients without a dynamic CT, and we focused on comparing LI-RADS categorization using Gd-DTPA-MRI and Gd-EOB-MRI.

Methodology
- retrospective
- observational
- performed at one institution

References

1. Sohrabpour AA, Mohamadnejad M, Malekzadeh R (2012) Review article: the reversibility of cirrhosis. Aliment Pharmacol Ther 36: 824–832
2. Bruix J, Sherman M, American Association for the Study of Liver D (2011) Management of hepatocellular carcinoma: an update. Hepatology 53:1020–1022
3. Mitchell DG, Bruix J, Sherman M, Sirlin CB (2015) LI-RADS (Liver Imaging Reporting and Data System): summary, discussion, and consensus of the LI-RADS Management Working Group and future directions. Hepatology 61:1056–1065
4. Hope TA, Fowler KJ, Sirlin CB et al (2015) Hepatobiliary agents and their role in LI-RADS. Abdom Imaging 40:613–625
5. Yu MH, Kim JH, Yoon JH et al (2014) Small (</=1-cm) hepatocellular carcinoma: diagnostic performance and imaging features at gadoxetic acid-enhanced MR imaging. Radiology 271:748–760
6. Ichikawa T, Saito K, Yoshioka N et al (2010) Detection and characterization of focal liver lesions: a Japanese phase III, multicenter

comparison between gadoxetic acid disodium-enhanced magnetic resonance imaging and contrast-enhanced computed tomography predominantly in patients with hepatocellular carcinoma and chronic liver disease. Invest Radiol 45:133–141
7. Kim JE, Kim SH, Lee SJ, Rhim H (2011) Hypervascular hepatocellular carcinoma 1 cm or smaller in patients with chronic liver disease: characterization with gadoxetic acid-enhanced MRI that includes diffusion-weighted imaging. AJR Am J Roentgenol 196: W758–W765
8. Choi SH, Byun JH, Lim YS et al (2016) Diagnostic criteria for hepatocellular carcinoma 3 cm with hepatocyte-specific contrast-enhanced magnetic resonance imaging. J Hepatol 64:1099–1107
9. An C, Rhee H, Han K et al (2016) Added value of smooth hypointense rim in the hepatobiliary phase of gadoxetic acid-enhanced MRI in identifying tumor capsule and diagnosing hepatocellular carcinoma. Eur Radiol. https://doi.org/10.1007/s00330-016-4634-6
10. Lee JM, Park JW, Choi BI (2014) 2014 KLCSG-NCC Korea Practice Guidelines for the management of hepatocellular carcinoma: HCC diagnostic algorithm. Dig Dis 32:764–777
11. Kudo M, Matsui O, Izumi N, Iijima H, Kadoya M, Imai Y (2014) Surveillance and diagnostic algorithm for hepatocellular carcinoma proposed by the Liver Cancer Study Group of Japan: 2014 update. Oncology 87(Suppl 1):7–21
12. Joo I, Lee JM, Lee DH, Ahn SJ, Lee ES, Han JK (2017) Liver imaging reporting and data system v2014 categorization of hepatocellular carcinoma on gadoxetic acid-enhanced MRI: Comparison with multiphasic multidetector computed tomography. J Magn Reson Imaging 45:731–740
13. Cha DI, Jang KM, Kim SH, Kang TW, Song KD (2017) Liver Imaging Reporting and Data System on CT and gadoxetic acid-enhanced MRI with diffusion-weighted imaging. Eur Radiol. https://doi.org/10.1007/s00330-017-4804-1
14. Choi SH, Byun JH, Kim SY et al (2016) Liver Imaging Reporting and Data System v2014 With Gadoxetate Disodium-Enhanced Magnetic Resonance Imaging: Validation of LI-RADS Category 4 and 5 Criteria. Invest Radiol 51:483–490
15. Bae JS, Kim JH, Yu MH et al (2017) Diagnostic accuracy of gadoxetic acid-enhanced MR for small hypervascular hepatocellular carcinoma and the concordance rate of Liver Imaging Reporting and Data System (LI-RADS). PLoS One 12:e0178495
16. Kim YN, Song JS, Moon WS, Hwang HP, Kim YK (2017) Intraindividual comparison of hepatocellular carcinoma imaging features on contrast-enhanced computed tomography, gadopentetate dimeglumine-enhanced MRI, and gadoxetic acid-enhanced MRI. Acta Radiol. https://doi.org/10.1177/0284185117728534:284185117728534
17. Lee YJ, Lee JM, Lee JS et al (2015) Hepatocellular carcinoma: diagnostic performance of multidetector CT and MR imaging-a systematic review and meta-analysis. Radiology 275:97–109
18. Golfieri R, Grazioli L, Orlando E et al (2012) Which is the best MRI marker of malignancy for atypical cirrhotic nodules: hypointensity in hepatobiliary phase alone or combined with other features? Classification after Gd-EOB-DTPA administration. J Magn Reson Imaging 36:648–657
19. Granito A, Galassi M, Piscaglia F et al (2013) Impact of gadoxetic acid (Gd-EOB-DTPA)-enhanced magnetic resonance on the noninvasive diagnosis of small hepatocellular carcinoma: a prospective study. Aliment Pharmacol Ther 37:355–363
20. Joo I, Lee JM, Lee DH, Jeon JH, Han JK, Choi BI (2015) Noninvasive diagnosis of hepatocellular carcinoma on gadoxetic acid-enhanced MRI: can hypointensity on the hepatobiliary phase be used as an alternative to washout? Eur Radiol 25:2859–2868
21. Zhang YD, Zhu FP, Xu X et al (2016) Liver Imaging Reporting and Data System:: Substantial Discordance Between CT and MR for Imaging Classification of Hepatic Nodules. Acad Radiol 23:344–352
22. Joo I, Kim H, Lee JM (2015) Cancer stem cells in primary liver cancers: pathological concepts and imaging findings. Korean J Radiol 16:50–68